Available online at www.sciencedirect.com
ScienceDirect
Journal of Controlled Release 128 (2008) 80–88
journal of controlled release
www.elsevier.com/locate/jconrel

Improved piercing of microneedle arrays in dermatomed human skin by an impact insertion method

F.J. Verbaan [a], S.M. Bal [a], D.J. van den Berg [a], J.A. Dijksman [b], M. van Hecke [b], H. Verpoorten [a], A. van den Berg [c], R. Luttge [d], J.A. Bouwstra [a,*]

[a] Department of Drug Delivery Technology, Leiden/Amsterdam Center for Drug Research, P.O. Box 9502, 2300 RA, Leiden, The Netherlands
[b] Kamerlingh Onnes Laboratory, Leiden University, P.O. Box 9504, 2300 RA Leiden, The Netherlands
[c] BIOS Lab-on-a-chip group, MESA+ Institute for Nanotechnology, University of Twente, P.O. Box 217, 7500 AE, Enschede, The Netherlands
[d] Mesoscale Chemical Systems, MESA+ Institute for Nanotechnology, University of Twente, P.O. 217, 7500 AE Enschede, The Netherlands

Received 12 November 2007; accepted 18 February 2008
Available online 26 February 2008

Abstract

An electrical applicator was designed, which can pierce short microneedles into the skin with a predefined velocity. Three different shapes of microneedles were used, namely 300 μm assembled hollow metal microneedle arrays, 300 μm solid metal microneedle arrays and 245 μm hollow silicon microneedle arrays. The latter are available as 4×4, 6×6 and 9×9 arrays.

When using a velocity of 1 or 3 m/s reproducible piercing of dermatomed and full thickness human skin was evident from the appearance of blue spots on the dermal side of the skin after Trypan Blue treatment and the presence of fluorescently labeled particles in dermatomed skin. Manual piercing did not result in the appearance of blue spots. Transport studies revealed that i) piercing of microneedles with a predefined velocity into human skin resulted in a drastic enhancement of the Cascade Blue (CB, Mw 538) transport, ii) A higher piercing velocity resulted in a higher CB transport rate, iii) The CB transport rate was also dependent on the shape of the microneedles and iv) no difference in transport rate was observed between 4×4, 6×6 and 9×9 hollow silicon microneedle arrays.

Keywords: Microneedles; Electric applicator; In vitro transport; Human skin

1. Introduction

The natural function of the skin is to protect the body against undesired influences from the environment. However, the skin barrier function is a major challenge for delivery of drugs via the skin. The barrier function is located in the outermost layer of the skin, the stratum corneum (SC), which consists of dead cells embedded in lipid regions. The SC thickness is only 10–20 μm.

One of the methods to bypass the skin barrier is the use of microneedle arrays [1,2]. As microneedles are designed to be painless, ideally they should protrude the SC and reach the viable epidermis, but not reach the dermis as in this region the nerve endings are located [3]. In order to achieve this, microneedles should be short and should penetrate the skin in a reproducible manner. However, in order to achieve this, one of the major challenges is to overcome the elasticity of the skin, which counteracts the penetration of short (i.e. less than 300 μm) microneedles into the skin as reported in previous papers: the skin is folded around the microneedle and piercing of the skin does not or only partially occur [4–7]. The effect of the flexibility of skin on the penetration of microneedles is scarcely addressed in literature. Until now, most publications concerning microneedles have dealt with the application of microneedles in vitro using human epidermal sheets or in vivo in mice or rats [7–10]. Both the epidermal human sheets and the skin of mice and rats are much thinner than human skin and it is therefore questionable whether microneedle penetration properties are similar to that in human skin in vivo.

* Corresponding author. Tel.: +31 715274208; fax: +31 715274565.
E-mail address: Bouwstra@chem.leidenuniv.nl (J.A. Bouwstra).

0168-3659/$ - see front matter © 2008 Elsevier B.V. All rights reserved.
doi:10.1016/j.jconrel.2008.02.009

Previously, we described the use of assembled hollow metal microneedle arrays to bypass the barrier function of dermatomed human skin in vitro. The microneedle arrays were made from commercially available hypodermic needles, and have microneedle lengths of 550, 700 and 900 μm. Pretreatment of human skin with these assembled hollow metal microneedles resulted not only in the delivery of small compounds, but also large molecules such as high molecular weight dextrans. However, in these studies we were not able to pierce the skin with microneedles of 300 μm length due to the elasticity of the skin resulting in a folding of the skin around the microneedle tip [6]. Recently, this skin folding has been visualized by Martanto et al. [4].

A means to improve the piercing of skin and create the possibility to use shorter microneedles and therefore make piercing more reproducible is the use of an impact insertion system that pierces the skin with a certain velocity circumventing the elasticity of the skin. Therefore, in this study we examined systematically the use of an electrically driven applicator to pierce human skin with a velocity that can be tailored. The beneficial effect of the applicator is demonstrated in vitro by the ability to pierce human skin in vitro by visual inspection using the Trypan Blue dye and by performing transdermal transport studies. As the microneedle number and microneedle density in the arrays might also affect the piercing of the skin, not only the microneedle length, but also the microneedle number and density were varied. For the transdermal transport cascade blue with a molecular weight of 538 Da, cascade blue was used. The results of the present study show that short (i.e. $\leq$300 μm) microneedle arrays are able to pierce dermatomed human skin in vitro by application with an electrically driven applicator.

2. Materials and methods

2.1. Materials

Cascade Blue (CB, Mw 538) was purchased from Invitrogen (Breda, The Netherlands). All other chemicals were from Sigma–Aldrich (Zwijndrecht, The Netherlands). The solid metal microneedle arrays were kindly provided by Transferium (Almelo, The Netherlands).

2.2. Microneedle array fabrication

In this study we used three types of microneedle arrays.

1. Assembled hollow metal microneedle arrays were manufactured from commercially available 30G hypodermic needles. As such, the individual microneedles have a diameter of about 300 μm and a length tailored to 300 μm. The microneedles are hollow [6]. The pitch of the microneedles is 1.25 mm, resulting in a microneedle array with a surface of 16.4 mm^2. The tapered shaft length (beveled edge) of these hypodermic needles is approximately 1.2 mm, which results in a very sharp tip. The microneedles were fixed in a polyetherketone mold as described before [6].
2. Solid metal microneedle arrays were assembled from stainless steel wire with a diameter of 200 μm and a length of 300 μm. The individual microneedles were cut tangentially to obtain sharp tips. The microneedles were fixed in a polyetheretherketone mold, similar as the assembled microneedle arrays. The pitch between the solid microneedles is also 1.25 mm. The tapered shaft of the solid needles has a length of approximately 200 μm (beveled tip with an angle of 45°), resulting in a less sharp tip than those of the hypodermic needles.
3. Hollow silicon microneedles with a length of about 245 μm were fabricated by combining surface micromachining and silicon etching [11]. The microneedles are 245 μm in length with a triangular tip shape, a base of 250 μm, and a maximum hole width of 70 μm. The center of the elliptical hole in the needle is positioned ca. 40 μm from the tip of the needle. The microneedles are positioned in a 5 by 5 mm^2 area. The microneedle number varied between 4×4, 6×6 and 9×9, which also results in a variation in microneedle density in the arrays.

In order to compare the microneedles in their ability to pierce human skin we used the various types of microneedles to pretreat the skin, after which we immediately applied the formulation of interest onto the skin surface. This is described in more details below.

2.3. Design of an electrically driven applicator

An electrically driven applicator with the ability to insert the microneedles with a high speed was designed. The slender device is approximately 20 cm long with an approximately 2 cm diameter at the tip. An array of microneedles is positioned at the end of the applicator and held in place by a metal holder shaped in the form of the mold of the microneedle arrays, which is protected by a Perspex cover. The device contains a coil through which current can be passed, resulting in a magnetic driving force allowing a metal rod to be pushed out of the coil, moving the attached microneedle array. The applied voltage can be varied between 24 and 60 V, using a custom made power supply varying the magnetic driving force (and thus insertion speed) accordingly. We utilized a high speed camera with a known frame rate to visualize the movement of the microneedle array from which the speed of the microneedle array could be calculated.

For manual piercing a hand-held applicator was used that has been described previously [6].

2.4. Preparation of human skin

Abdominal or breast skin was obtained from local hospitals following cosmetic surgery and was used within 24 h after surgery. Full thickness skin was prepared by removing residual subcutaneous fat using a surgical scalpel. The stratum corneum side was carefully wiped with 70% ethanol and deionised water.

Dermatomed human skin was prepared by fixing full thickness skin on a styrofoam support and the skin was dermatomed to a thickness of 300–400 μm using a Padgett Electro Dermatome Model B (Kansas City, USA) as described by Nugroho et al. [12]. The skin was stored at −80 °C until use,

except for transport and confocal studies where only fresh human skin was used.

2.5. Piercing of human skin and visual inspection in vitro

Full thickness skin or dermatomed human skin was stretched on parafilm to counteract the elasticity of the skin. Subsequently, the skin was supported by styrofoam to protect the microneedles from damage and pierced using the electrically driven applicator. Then the skin was immediately used either for the visualization studies or for the diffusion studies. Visualization studies were performed macro- and microscopically after the skin had been pierced with the applicator using either a velocity of 3 m/s or by manual piercing of the skin. To evaluate the uniformity of piercing, the SC-side of the pierced skin was covered with 0.4% Trypan Blue dye in phosphate buffer saline (PBS: NaCl: 8 g/l, KCl: 0.4 g/l, KH2PO4: 0.4 g/l, Na2HPO4: 2.86 g/l) for 1 h. Full thickness skin was first dermatomed to a thickness of 300–400 μm before application of the Trypan Blue dye. The excess dye was then removed and the skin or epidermal sheet was evaluated for the appearance of blue dots on the dermal side of the skin or epidermal sheets.

2.6. Confocal studies

To visualize the conduits in dermatomed human skin, we applied polystyrene nanoparticles (FluoSpheres® carboxylate-modified nanoparticles, Invitrogen, Breda, The Netherlands) containing fluorescein 5-isothiocyanate with a size of 200 nm to human skin pretreated with the solid metal microneedle arrays using the electrical applicator. Piercing velocity was 1 or 3 m/s. After piercing the skin was placed in a Franz diffusion cell and 200 μL of a particle solution was applied for 1 h. Afterwards the excess formulation was removed from the skin surface and the skin was washed three times with phosphate buffer with a cotton swab. The skin was mounted on a sample holder and visualized with a confocal laser scanning microscope. Images were processed using a Bio-Rad Radiance 2100 confocal laser scanning system equipped with a Nikon Eclipse TE2000-U inverted microscope and a 20X S Fluor (NA 1.30; Nikon, Japan) air objective. The images were captured using argon laser at 488 nm wavelength, with a 515/30 nm emission filter. Image acquisition was controlled using the Laser Sharp 2000 software (Bio-Rad, Hercules, USA).

2.7. Diffusion studies

In vitro transport studies were performed in order to examine the effect of microneedle pretreatment on the permeation of CB across dermatomed human skin. CB was selected as this dye was also used in our previous studies [6], in which we compared the efficiency of piercing for trandermal delivery of substances varying over a wide range of molecular weights. Transport studies were performed after the following pretreatments:

a. Variation in microneedle arrays: 4×4 solid metal microneedle arrays, 4×4 assembled hollow metal microneedle arrays or 4×4 hollow silicon microneedle arrays. The microneedles were pierced into the skin with a velocity of 3 m/s.
b. Variation in velocity of the microneedles when piercing the skin. Manual application, 1 m/s velocity and 3 m/s velocity of the microneedles when piercing the skin was compared.
c. Variation in microneedle density and number: a comparison between 4×4, 6×6 and 9×9 hollow silicon microneedles.
d. Stripped dermatomed skin: Dermatomed human skin was clamped between two circular plates fixed together with 4 screws. In the central part of upper plate, facing the stratum corneum side of the skin, a circular hole with a diameter of 1 cm was made to perform tape-stripping. Tape-stripping was carried out using an adhesive tape (Scotch® Magic™ Tape 810, 3 M France), which was pressed onto the skin for 5 s. Tape-strips were then rapidly pulled off with 1 fluent stroke. The direction of tape-stripping was alternated. Tape-stripping was continued until the viable epidermis was reached.

In vitro transport studies were performed as described by Grams and Bouwstra [13] using continuous flow-through diffusion cells (PermeGear, Inc., Bethlehem, USA). The diffusion area was 1.16 cm^2. After pretreatment with microneedle arrays, dermatomed human skin or stripped dermatomed human skin was placed between the donor compartment and receptor compartment with the SC side facing the donor compartment. A disk of wire gauze (Ø 18 mm) was used to support the dermatomed human skin. The acceptor phase was PBS (NaCl: 8 g/l,

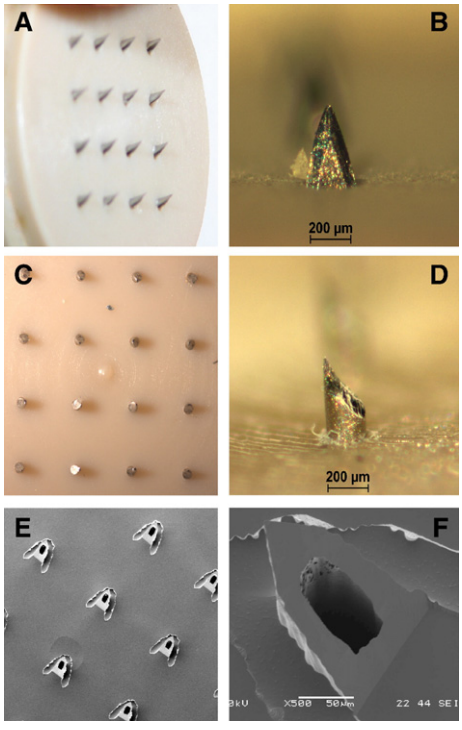

Fig. 1. The various microneedle arrays used in this study are i) commercially available (assembled) hollow metal needles in a 4×4 array (A) and a higher magnification of a single microneedle (B), solid metal microneedle arrays in a 4×4 array (C) and a higher magnification of a single solid microneedle (D), and iii) SEM images of hollow silicon 4×4 microneedle array (E) and a higher magnification (F).

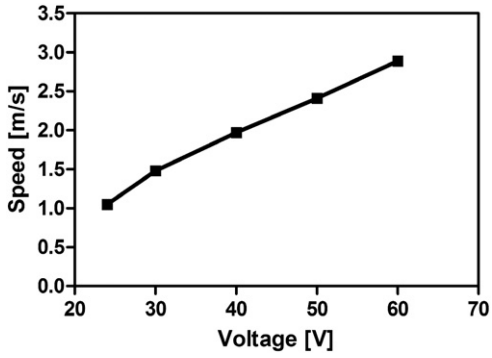

Fig. 2. The velocity of the microneedles using the electrically driven applicator: The velocity is linearly related to the applied voltage.

KCl: 0.4 g/l, KH_2PO_4: 0.4 g/l, Na_2HPO_4: 2.86 g/l) and was kept at 37 °C resulting in a skin surface temperature of approximately 32 °C in the diffusion cell. The donor solutions contained 0.2 mM cascade blue in PBS. The volume applied was 1 ml. The flow rate of the PBS in the acceptor chamber was maintained at approximately 1 ml/h by a peristaltic pump (Ismatec SA, Glattbrugg, Switzerland). The donor compartment was covered with 3 M scotch tape to establish occlusive conditions. Hourly fractions of the acceptor phase were collected over a period of 20 h and analyzed by HPLC.

2.8. Analysis by HPLC

The concentration of CB was determined by injecting 10 µl of sample on a Waters HPLC system consisting of a Waters 600 controller coupled to a Waters 717 plus auto sampler and a Waters 474 Scanning Fluorescence Detector (Waters Chromatography B.V., Etten-Leur, The Netherlands) and a column Inertsil, 5 µm, ODS-3, 250 mm × 3 mm (Varian B.V., Middelburg, The Netherlands). Excitation and emission wavelengths of 401 and 431 nm were used. PBS was used as the mobile phase at a flow rate of 1 ml/min.

3. Results

3.1. Microneedles

Assembled hollow metal microneedle arrays prepared from 30G needles having a length of 300 µm are depicted in Fig. 1A and B. The solid metal microneedle arrays (300 µm in length) are shown in Fig. 1C and D. Fig. 1E and F shows a scanning electron microscopy image of a hollow silicon microneedle array with a triangular tip shape base of 270 µm and a maximal hole width of 70 µm. The length of a single microneedle is 245 µm.

3.2. Applicator design: speed variation

The speed with which the microneedles can be moved by the applicator was measured using a high speed camera with a known frame rate to visualize the movement of the microneedle array from which the speed of the microneedle array could be calculated. Fig. 2 shows that the speed can be varied linearly from about 1 to 3 m/s corresponding to 24 V to 60 V, respectively.

3.3. In vitro evaluation of piercing human skin

Dermatomed skin: To study piercing, microneedles were applied to the SC side of dermatomed skin using the electrically driven applicator. The microneedles were pierced into the skin with a velocity of 3 m/s or 1 m/s or manually with the previously described hand-held applicator [6]. Using the manual and the electrical applicator, the angle between microneedle core and the skin was 90°. Then Trypan Blue dye formulation was spread over the pierced site. The presence of conduits in the skin was visualized by the appearance of blue dots at the dermal side. Fig. 3 shows that for all types of microneedle arrays, blue dots are formed when they are applied with the electrically driven applicator. Furthermore, not only 4 × 4, but also 6 × 6 and 9 × 9 hollow silicon microneedle arrays were able to pierce dermatomed human skin. Only a few blue spots appeared when

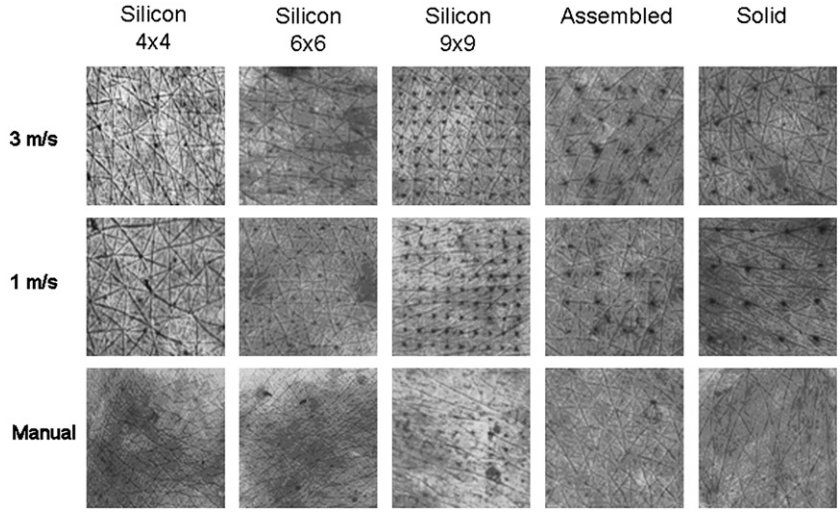

Fig. 3. Piercing of assembled 4 × 4 hollow metal microneedle arrays, 4 × 4 solid metal microneedle arrays and 4 × 4, 6 × 6 and 9 × 9 hollow silicon microneedle arrays across dermatomed human skin when applied with a velocity of 1 m/s, 3 m/s or manually. Piercing was visualized with the Trypan blue assay.

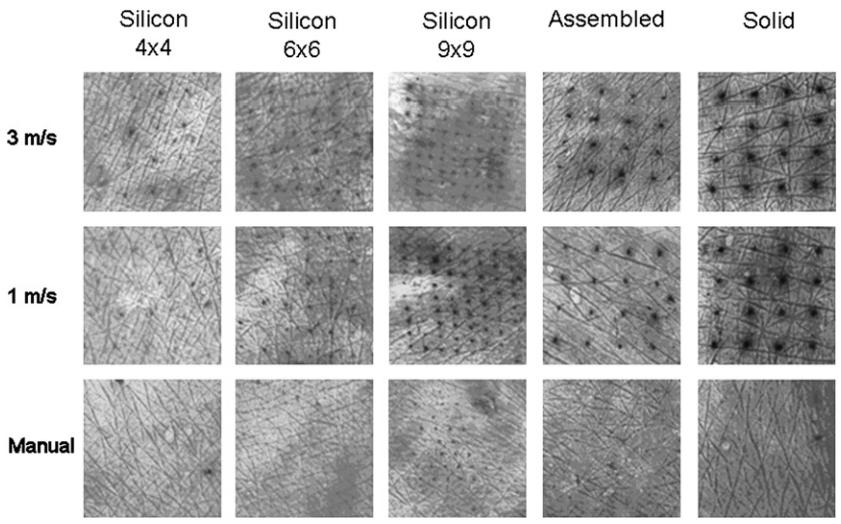

Fig. 4. Piercing of assembled 4×4 hollow metal microneedle arrays, 4×4 solid metal microneedle arrays and 4×4, 6×6 and 9×9 hollow silicon microneedle arrays across full thickness human skin when applied with a velocity of 1 m/s, 3 m/s or manually. Piercing was visualized with the Trypan blue assay.

dermatomed human skin was pierced manually with the same microneedle arrays. These results demonstrate that the electrically driven applicator has superior piercing properties compared to the manual applicator.

Full thickness human skin: To study the effect of skin thickness on the piercing into the skin, we performed a similar experiment using full thickness human skin. Fig. 4 shows piercing of the skin with the short microneedles, similarly to dermatomed human skin, which again indicates that the electrically driven applicator is able to overcome the flexibility of the skin and has superior piercing properties compared to the manual applicator.

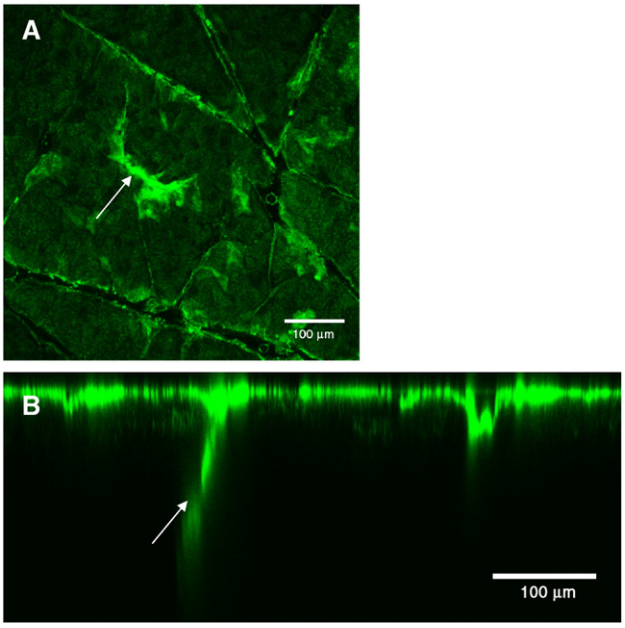

Fig. 5. Visualisation of the transport of 200 nm FITC-nanoparticles into human skin after microneedle array pretreatment. (A) x,y image (parallel to skin surface) showing localization of the nanoparticles in a conduit at a depth of 20 µm. Keratinocytes are also visible indicating the presence of viable epidermis at this depth. (B) x,z image (perpendicular to skin surface) shows penetration of the nanoparticles up to 250 µm into the skin. The conduit is indicated by an arrow. In Fig. 5B the irregular shape of the skin surface is due to the wrinkles in the skin.

3.4. Confocal studies

After microneedle pretreatment conduits are present in the skin. Fluorescent nanoparticles with a size of 200 nm were able to enter these conduits. Fig. 5 shows that nanoparticles are present in the conduits. Also some fluorescence from the wrinkles can be observed. The conduits are moon-shaped and have a depth of approximately 250 µm (Fig. 5B). No difference in penetration depth of the nanoparticles was observed between piercing the microneedles with a velocity of 1 and 3 m/s (not shown).

3.5. Transport studies using the electrically driven applicator

Transport studies were performed in order to study the effect of i) piercing velocity of the microneedles into the skin, ii) the microneedle shape and iii) the number of microneedles in the array. As model compound CB with a molecular weight of 538 was used.

Piercing velocity of the microneedles: The transport of CB was determined after pretreatment of dermatomed human skin with assembled hollow metal microneedle arrays, solid metal microneedle arrays and hollow silicon microneedle arrays, which were inserted into the skin with two different insertion velocities (1 and 3 m/s). Insertion of microneedles using the manual applicator was performed as a comparison. For all situations, the control skin (i.e. no microneedle array pretreatment) resulted in non-detectable fluxes as shown in Fig. 6. Manual pretreatment with microneedle arrays resulted in a slight but significant increase in the flux of CB, indicating that some of the short microneedles protruded the dermatomed human skin when applied manually. However, very interestingly, for all microneedle arrays, pretreatment with microneedle arrays applied by the electrically driven applicator resulted in a

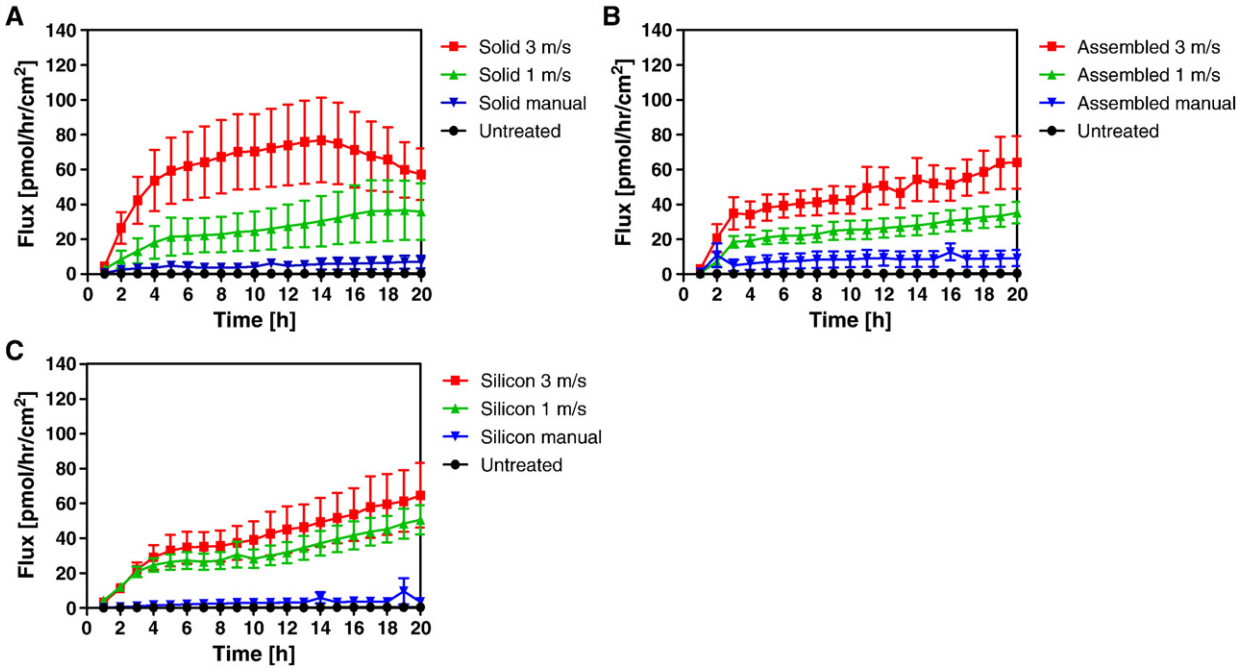

Fig. 6. Transport of CB after pretreatment of dermatomed human skin with 4×4 solid metal microneedle arrays (A), 4×4 assembled hollow metal microneedle arrays (B) and 4×4 silicon hollow microneedle arrays (C) pierced through the skin with a velocity of 3 m/s, 1 m/s or manually. Data are presented as averages±SEM, Each curve is at least 6 replicas of at least three donors.

drastic increase in transport of the compound across dermatomed human skin. The obtained CB fluxes (see Table 1) were higher after insertion with a velocity at 3 m/s compared to an insertion velocity of 1 m/s. The difference, however, was less pronounced for the hollow silicon microneedles compared to the assembled hollow metal microneedle arrays and the solid metal microneedle arrays. As far as the shape of the flux curves is concerned after an initial period of 2–4 h there is still a gradual increase in transport, except for the pretreatment of the solid metal microneedles inserted at 3 m/s, where the transport rate was slightly reduced after 12 h (see Fig. 6).

Type of microneedle array: When comparing the 4×4 assembled hollow metal microneedle arrays, the 4×4 solid metal microneedle arrays and the 4×4 hollow silicon microneedle arrays, it is clearly demonstrated that besides the

Table 1
CB mean fluxes±s.e.m. between 11 and 20 h expressed in pmol/cm^2/h

Microneedle arrays	Velocity (m/s)	Mean flux±s.e.m.
4×4 Solid metal	M*	6±3
4×4 Solid metal	1	44±17
4×4 Solid metal	3	70±21
4×4 assembled hollow metal	M*	9±4
4×4 assembled hollow metal	1	30±6
4×4 assembled hollow metal	3	55±11
4×4 hollow silicon	M*	4±2
4×4 hollow silicon	1	41±8
4×4 hollow silicon	3	54±16
6×6 hollow silicon	3	48±12
9×9 hollow silicon	3	68±26
Untreated skin		0.4±0.2

*M= manually piercing.

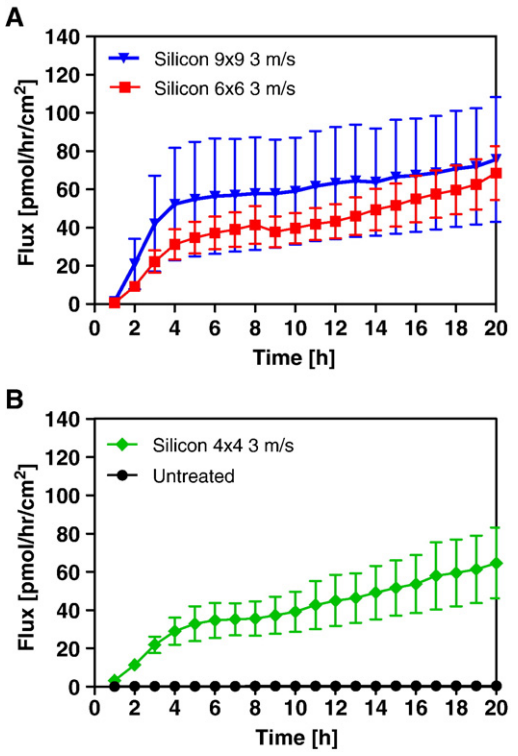

Fig. 7. Transport of CB after pretreatment of dermatomed human skin with (A) 6×6 or 9×9 hollow silicon microneedle arrays. (B) 4×4 silicon microneedle arrays and control (no piercing). The piercing velocity is 3 m/s. Data are presented as averages±SEM, Each curve is at least 6 replicas of at least three donors.

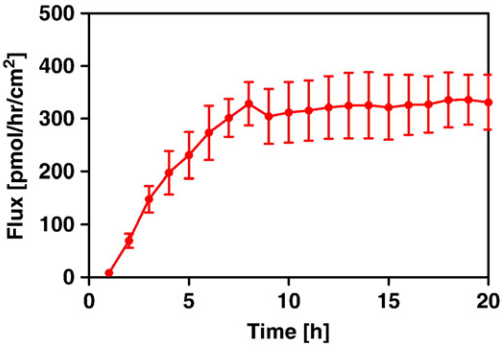

Fig. 8. Transport of CB after pretreatment of dermatomed human skin after removing the stratum corneum by stripping. Data are presented as averages ± SEM, The experimental data are based on 4 replicas of two donors.

insertion speed, the shape of the arrays also determines the CB transport rate across the dermatomed human skin. The solid metal microneedle arrays resulted in much higher fluxes than the assembled and the hollow silicon microneedle arrays, see Fig. 6.

Microneedle array density and stripped dermatomed human skin: The effect of microneedle density and number of microneedles on the transport of CB was also studied and compared to stripped dermatomed skin. In our transport studies we used 4×4, 6×6 and 9×9 hollow silicon microneedle arrays. The fluxes of the 4×4, 6×6 and 9×9 hollow silicon microneedle arrays were all significantly increased compared to the untreated situation when the microneedle arrays were applied with the electrical applicator (Fig. 7). There was no statistically significant difference, however, between the 4×4, 6×6 and 9×9 hollow silicon microneedles, although pretreatment with the 9×9 microneedle arrays results in the highest CB fluxes. Hence, the increase in number of microneedles and microneedle density in the arrays did not result in a significantly increase in the CB transport rate across the skin. To determine the maximum CB transport the flux across stripped dermatomed human skin was also examined. The results are provided in Fig. 8. The stripped dermatomed skin resulted in very high fluxes of CB.

4. Discussion

In this study, we showed that the use of an impact insertion system greatly facilitates the insertion of microneedle arrays with short length (i.e. ≤300 μm) into dermatomed human and full thickness human skin in vitro.

Microfabrication techniques for the production of silicon, metal, glass and polymer microneedle arrays with micrometer dimensions have been described. Production of microneedles often is highly specialized and includes complex multi-step processes [14–18]. Very recently several studies were reported in which coated microneedles were designed [19–21]. In the present study we used 4×4 microneedle arrays from commercially available 30G hypodermic needles or stainless steel wire and compared the effect on transport studies with silicon arrays fabricated by micromachining combined with etching techniques. Fabrication of microneedles prepared from stainless steel wire can also be modified for mass production and is therefore important to investigate. Furthermore, very recently, in an in vivo study solid and assembled microneedle arrays have been investigated for pain sensation and skin irritation in humans. Skin irritation as well as pain sensation appeared to be minimal [22], which makes them even more suitable for percutaneous administration of drug or vaccine. The 30G hypodermic needles and the solid metal microneedles are fixed on a backplate forming arrays having a needle length of 300 μm. While the 30G hypodermic needles are very sharp with a long shaft of approximately 1.2 mm, the length of the shaft of the solid metal microneedles is around 280 μm. The tip shape of the latter is triangular with an angle of approximately 45°. The hollow silicon microneedles arrays have also a triangular tip and varied in microneedle density. For this study we had available 4×4, 6×6 and 9×9 hollow silicon microneedle arrays as described by Gardeniers et al. [11], fabricated on a 5 mm×5 mm surface area. Therefore the 9×9 microneedle density is much higher than the 4×4 microneedle density.

In a recent paper we showed that using a manual application, piercing of microneedles with a length of 300 μm was not successful, while piercing was possible with microneedle lengths of 550 μm and longer [6]. This was observed both, in vitro using dermatomed human skin and in vivo in humans. Therefore, for piercing properties of microneedles dermatomed human skin acts as an acceptable model for in vivo studies in humans. As the needle length required for piercing is much longer than the thickness of the stratum corneum, it was postulated that the elasticity of the skin counteracted the penetration of microneedles into the skin when they were inserted slowly into the skin. The effect of the elasticity of the skin on the piercing ability of microneedles has also elegantly been demonstrated by Martanto et al. [4]. As there is an inter individual and intra individual variation of the elasticity of the skin, in which for example age and skin region play an important role, the effect of the elasticity of the skin makes piercing less reproducible. For this reason we decided to design a novel applicator, which allows the insertion of microneedles into the skin with a fixed predetermined velocity. As is very clear from Figs. 3 and 4, using a velocity of only 3 m/s, microneedles with a length of 245 μm or 300 μm were inserted into the skin in a very reproducible manner, which contrasted the results with the manual applicator. Therefore, not only microneedle length, but also the speed of insertion drastically affects piercing properties of the microneedle arrays. In these piercing studies we did not observe any difference in piercing ability between the differently shaped microneedles. In other words, piercing of the 30G hypodermic needles with a very sharp tip was very similar to that of the silicon and solid microneedles with a less sharp tip. Using a velocity of 1 m/s and 3 m/s piercing of microneedles occurred as also demonstrated by the confocal studies. Furthermore, not only the 4×4, but also the 6×6 and 9×9 microneedle arrays with a needle length of only 245 μm were able to pierce the skin. This is of interest, as a higher microneedle density might counteract the piercing ability due to different pressures at the tip of the microneedles, resulting in difference in piercing properties (i.e. bed of nails

effect). From these piercing studies the beneficial effects of the electric applicator is already obvious. In a previous study, hollow silicon microneedles were also used successfully in piercing the skin. However, in that report no experimental details are provided about the piercing studies and the use of an applicator [11]. In our studies taking into account that the total weight of the moving part of applicator and the microneedle arrays is 0.0115 kg, the obtained kinetic energy when reaching the skin with a velocity of 1 or 3 m/s is 0.0058 J and 0.052 J, respectively. These kinetic energies are by far sufficient to pierce the skin assuming a flat tip size (solid metal microneedles) of approximately 600 μm^2 and the puncture toughness of around 30 kJ/cm^2 as published previously [23,24]. This is in agreement with the piercing studies.

In order to study the effect of microneedle insertion velocity on the piercing ability in more detail transport studies were performed using the model drug CB. Two insertion velocities were used to pretreat dermatomed human skin, namely 1 and 3 m/s. From these studies it is obvious that a higher insertion velocity results in a higher transport rate. This is observed for the three types of microneedle arrays used in this study. Furthermore, even an insertion velocity of only 1 m/s already resulted in a drastic increase in the transport rate compared to the manual application. When comparing the effect of the different microneedle arrays on the transport rate of CB, it is clear that the solid metal microneedle array pretreatment results in significant higher fluxes than the assembled and hollow silicon microneedle array pretreatment. This shows that in addition to the insertion velocity, indeed, the shape of the microneedles also affects the transport across the skin. One can speculate that in case of the solid metal microneedle arrays, due to the less sharp tip, the protrusions in the skin are somewhat larger than in case of the assembled hollow metal microneedle arrays, which might result in higher transport rates. Furthermore, the solid microneedle arrays are somewhat longer than the silicon microneedles, which might also be an advantage for increasing the transport across the skin. In additional studies the microneedle density on the transport rate was evaluated. These studies revealed no significant difference in flux between 4×4, 6×6 and 9×9 silicon microneedle arrays. The silicon microneedles used in this study have fixed array areas. Therefore, differences in needle density may cause differences in piercing properties as explained above and therefore the higher density microneedles may leed to a less deep piercing into the skin. Since the microneedles are also tapered, the resulting diameter of the conduit in the skin may be less when using the 9×9 microneedle arrays then using the 4×4 microneedle arrays. Another explanation may be that the number of microneedles used in this study is already too large to observe difference in steady state fluxes as proposed by Wu et al. [25] and recently also by Davis et al. [23]. Wu et al. [25] showed that beyond a certain number of microneedles there is only little increase in flux, as the relative reduction in skin resistance for diffusing molecules after each additional microneedle piercing is decreased. This might also explain why the transport across stripped skin is only a factor 6–7 higher (see Fig. 8) compared to that across solid microneedle pretreated skin, while the area of stratum corneum "removal" after microneedle treatment is only 0.45% of that of the stripped skin.

5. Conclusion

As evident from the visual inspection of pierced skin, appearance of blue spots after Trypan Blue application and passive transport studies, the formation of conduits by short microneedle arrays (i.e. ≤ 300) is dramatically improved in vitro by insertion using an impact insertion system. This system is able to insert the short microneedles with an insertion velocity of 1 and 3 m/s into dermatomed and full thickness human skin.

Acknowledgments

This work is financially supported by the Dutch Science & Technology Foundation (STW), project number LPG.5950. We like to thank Transferium (Almelo, The Netherlands) for providing the solid microneedle arrays.

References

[1] S. Henry, D.V. McAllister, M.G. Allen, M.R. Prausnitz, Microfabricated microneedles: a novel approach to transdermal drug delivery, J. Pharm. Sci. 87 (1998) 922–925.
[2] S. Kaushik, A.H. Hord, D.D. Denson, D.V. McAllister, S. Smitra, M.G. Allen, M.R. Prausnitz, Lack of pain associated with microfabricated microneedles, Anesth. Analg. 92 (2001) 502–504.
[3] G.F. Odland, in: L.A. Goldsmith (Ed.), Physiology, Biochemistry and Molecular Biology of the skin, vol. I, Oxford University Press, 1991, pp. 3–63.
[4] W. Martanto, J.S. Moore, T. Couse, M.R. Prausnitz, Mechanism of fluid infusion during microneedle insertion and retraction, J. Control. Release 112 (3) (May 30 2006) 357–361.
[5] W. Martanto, J.S. Moore, O. Kashlan, R. Kahmat, P.M. Wang, J.M. O'Neal, M.R. Prausnitz, Microinfusion using hollow microneedles, Pharm. Res. 23 (2006) 104–113.
[6] F.J. Verbaan, S.M. Bal, D.J. van den Berg, W.H. Groenink, H. Verpoorten, R. Luttge, J.A. Bouwstra, Assembled microneedle arrays enhance the transport of compounds varying over a large range of molecular weight across human dermatomed skin, J. Control. Release 117 (2007) 238–245.
[7] Y. Ito, J. Yoshimitsu, K. Shiroyara, N. Sugioka, K. Takada, Self-dissolving microneedles for the percutaneous absorption of EPO in mice, J. Drug Target. 14 (2006) 255–261.
[8] F. Chabri, K. Bouris, T. Jones, D. Barrow, A. Hann, C. Allender, K. Brain, J. Birchall, Microfabricated silicon microneedles for nonviral cutaneous gene delivery, Br. J. Dermatol. 150 (2004) 869–877.
[9] S.A. Coulamn, D. Barrow, A. Anstey, C. Gateley, A. Morrissey, N. Wilke, C. Allender, K. Brain, J.C. Birchall, Invasive cutaneous delivery of macromolecules and plasmid DNA via microneedles, Curr. Drug Deliv. 3 (2006) 65–75.
[10] D.V. McAllister, P.M. Wang, S.P. Davis, J.H. Park, P.J. Canatella, M.G. Allen, M.R. Prausnitz, S. Kaushik, A.H. Hord, D.D. Denson, S. Smitra, S. Henry, Microfabricated needles for transdermal delivery of macromolecules and nanoparticles: fabrication methods and transport studies, Proc. Natl. Acad. Sci. U.S.A. 100 (2003) 13755–13760.
[11] H.J.G.E. Gardeniers, Regina Luttge, Erwin J.W. Berenschot, Meint J. de Boer, Shuki Y. Yeshurun, Meir Hefetz, Ronny van't Oever, Albert van den Berg, Silicon micromachined hollow microneedles for trandermal liquid transport, J. Microelectromechanical syst. 12 (2003) 855–861.
[12] A.K. Nugroho, G.L. Li, M. Danhof, J.A. Bouwstra, Transdermal iontophoresis of rotigotine across human stratum corneum in vitro: influence of pH and NaCl concentration, Pharm. Res. 21 (2004) 844–850.

[13] Y.Y. Grams, J.A. Bouwstra, Penetration and distribution of three lipophilic probes in vitro in human skin focusing on the hair follicle, J. Control. Release 83 (2002) 253–262.
[14] M.A. Teo, C. Shearwood, K.C. Ng, J. Lu, S. Moochhala, In vitro and in vivo characterization of MEMS microneedles, Biomed. Microdevices 7 (1) (2005) 47–52.
[15] J.H. Park, M.G. Allen, M.R. Prausnitz, Polymer microneedles for controlled-release drug delivery, Pharm. Res. 23 (5) (2006) 1008–1019.
[16] S.P. Davis, W. Martanto, M.G. Allen, M.R. Prausnitz, Hollow metal microneedles for insulin delivery to diabetic rats, IEEE Trans. Biomed. Eng. 52 (5) (2005) 909–915.
[17] B. Ziaie, A. Baldi, M. Lei, Y. Gu, R.A. Siegel, Hard and soft micromachining for BioMEMS: review of techniques and examples of applications in microfluidics and drug delivery, Adv. Drug Deliv. Rev. 56 (2004) 145.
[18] Y. Ito, J. Yoshimitsu, K. Shiroyama, N. Sugioka, K. Takada, Self-dissolving microneedles for the percutaneous absorption of EPO in mice, J. Drug Target. 14 (2006) 255–261.
[19] M. Cornier, B. Johnson, M. Ameri, Kofi Nyam, L. Libiran, D.D. Zhang, P. Daddona, Transdermal delivery of desmopressin using a coated microneedle array patch system, J. Control. Release 97 (2004) 503–511.
[20] H.S. Gill, M.R. Prausnitz, Coated microneedles for transdermal delivery, J. Control. Release 117 (2007) 227–237.
[21] H.S. Gill, M.R. Prausnitz, Coating Formulations for microneedles, Pharm. Res. 24 (2007) 1369–1380.
[22] S.M. Bal, J. Caussin, S. Pavel, J.A. Bouwstra. In vivo assessmenrt of safety of microneedle arrays in human skin. Eur. J. Pharm. Sci., submitted for publication.
[23] S.P. Davis, B.J. landis, Z.H. Adams, M.G. Allen, M.P. Prausnitz, Insertion of microneedles into skin: measurement and prediction of insertion force and needle fracture force, J. Biomech. 37 (2004) 1155–1163.
[24] P.P. Purslows, Measurement of the fracture toughness of extensible connective tissues, J. Mater. Sci. 18 (1983) 3591–3598.
[25] X.-M. Wu, H. Todo, K. Sugibayashi, Effects of pre-treatment of needle puncture and sandpaper abrasion on in vitro skin permeation of fluorescein isothiocyanante (FITC)-dextran, Int. J. Pharm. 316 (2006) 102–108.